Andean Geology 37 (2): 413-432. July, 2010

Andean Geology
formerly Revista Geológica de Chile
www.scielo.cl/andgeol.htm

On the presence of Upper Paleocene rocks in the foreland succession at Cabo Nariz, Tierra del Fuego, Chile: geology and new palynological and U-Pb data

Alejandro Sánchez[1], Polina Pavlishina[2], Estanislao Godoy[3*], Francisco Hervé[1], C. Mark Fanning[4]

[1] *Departamento de Geología, Universidad de Chile, Casilla 13518, Correo 21, Santiago, Chile.*
alsanche@cec.uchile.cl; fherve@cec.uchile.cl

[2] *Department of Geology and Palaeontology, Sofia University 'St. Kl. Ohridski', 1504 Sofia, Bulgaria.*
polina@gea.uni-sofia.bg

[3] *Servicio Nacional de Geología y Minería, Av. Santa Maria 0104, Santiago, Chile .*
egodyster@gmail.com

[4] *Research School of Earth Sciences, The Australian National University, Mills Road, Canberra, ACT 0200, Australia.*
mark.fanning@anu.edu.au

[*] *Present address: Virginia Subercaseaux 4100, Pirque, Chile.*

ABSTRACT. On the west coast of Tierra del Fuego, south of Cabo Nariz, in Chile, Upper Cretaceous to Paleocene sedimentary successions of the Magallanes foreland basin crop out. The presence of dinoflagellate cysts, as well as radiometric U-Pb SHRIMP dating of detrital zircons, indicate that this succession ranges from the Campanian to Thanetian (Late Paleocene) in age. The base of the exposed sedimentary succession comprises siltstones of external platform facies (Cerro Cuchilla Formation), which are thrust over the Cabo Nariz Beds. The latter formation is divided into two members: a lower siltstone-dominated turbidite facies member and an upper member of sandstone-dominated turbidites, with sandstone and conglomerate channel facies. The presence of dinocysts in the Cerro Cuchilla Formation suggests a late Campanian to early Danian age. The fossil content in the Cabo Nariz Beds indicate a Selandian (Middle Paleocene) depositional age in accordance with the detrital zircon ages which provide a maximum possible Campanian age (76.5±0.7 Ma), and very close to the Thanetian (Late Paleocene) (57.6±1 Ma) depositional ages for the lower and upper member, respectively. The sedimentary succession of Cabo Nariz Beds, is interpreted as a north-northwest prograding submarine fan of middle to Late Paleocene age. It is considered to represent the deposition of detritus derived from an uplifting orogen located to the south. The detrital zircon age spectra suggest that there was a period of low intensity of magmatic activity in the source area around the K-T boundary.

Keywords: Dinoflagellate cysts, K-T, Stratigraphy, U-Pb detrital zircon ages, Tierra del Fuego, Chile.

RESUMEN. Acerca de la presencia de rocas del Paleoceno Superior en la sucesión de antepaís de Cabo Nariz, Tierra del Fuego, Chile: geología y nuevos datos palinológicos y de U-Pb. En la costa occidental de Tierra del Fuego, al sur de Cabo Nariz, Chile, afloran sucesiones sedimentarias de antepaís cretácicas tardías a paleocenas de la cuenca de Magallanes. Tanto su contenido de dinoquistes como las edades de circones detríticos indican que comprenden un intervalo de edades entre el Campaniano tardío y el Thanetiano (Paleoceno Tardío). La base de la sucesión sedimentaria expuesta comprende limolitas de facies de plataforma externa (Formación Cerro Cuchilla), la cual cubre tectónicamente los estratos de Cabo Nariz. Estos últimos se dividen en dos miembros: uno inferior de facies turbidíticas con predominio de limolitas y un miembro superior también de facies turbidíticas, pero con predominio de areniscas y facies de canales ricos en areniscas y conglomerados. De acuerdo a la presencia de dinoquistes, la Formación Cerro Cuchilla tiene edades comprendidas entre el Campaniano tardío y el Daniano temprano. El contenido fosilífero de los estratos de Cabo Nariz, indica una edad deposicional selandiana (Paleoceno Medio), la cual concuerda con las edades máximas posibles de sedimentación dadas por las edades de circones detríticos, que es campaniana (76,5±0,7 Ma), y muy cerca del Thanetiano (Paleoceno Tardío) (57,6±1 Ma) para los miembros inferior y superior respectivamente. Las sucesiones sedimentarias de los estratos de Cabo Nariz son interpretadas como un sistema de abanico submarino que prograda hacia el norte-noroeste entre el Paleoceno Medio y Tardío. Este es considerado como un depósito de detritos proveniente desde un orógeno que se alzó al sur durante ese período. El intervalo de edades de los circones detríticos sugiere que hubo un período de baja intensidad de actividad magmática en el área fuente, en torno al límite K-T.

Palabras clave: Dinoquistes, K-T, Estratigrafía, Edades U-Pb circones detríticos, Tierra del Fuego, Chile.

1. Introduction

A thick succession of the Cretaceous-Cenozoic Magallanes Foreland Basin crops out in central Tierra del Fuego, Chile, trending northwest to southeast and across the island from the Magallanes Strait to the Atlantic coast. Uplift has exposed this succession along major faults ascribed to the Magallanes Fold and Thrust Belt (MFTB). The structures have an orientation that ranges between northwest-southeast to east-west approaching the Atlantic coast (Fig.1). The foreland sedimentary succession provides a record of the interplay between the MFTB evolution and sedimentation within a compressional basin.

Cabo Nariz, located on the western coast of Tierra del Fuego (Fig. 1), comprises part of the foreland successions and has been studied by geologists of the Empresa Nacional del Petróleo (Chile) (Céspedes, 1971[1]; Rojas *et al.*, 1993[2]), though precise age data is lacking in that area and their reports differ in the assignment of the units (Fig. 2). Céspedes (1971)[1] states that the Cerro Cuchilla Formation (Upper Cretaceous) structurally overlies the Agua Fresca Formation (Paleocene), which in turn overlies the Chorrillo Chico Formation (Paleocene) with a transitional contact, meanwhile, Rojas *et al.*(1993)[2] state that the Cerro Cuchilla Formation is overlain by the Cabo Nariz Formation (Agua Fresca Formation of Céspedes (1971)[1]). Furthermore, the Chorrillo Chico Formation of Céspedes (1971)[1] is assigned by Rojas *et al.*(1993)[2] to the upper part of the Cerro Cuchilla Formation (Fig. 2).

In this study, the main stratigraphic aspects of the units recognized in the Cabo Nariz area are presented, as well as dinoflagellate cyst determinations and SHRIMP U-Pb dating on detrital zircons. These new data allow a more precise age assignment for the succession, and consequently a new definition of stratigraphic units is proposed. Finally, a structural profile interpretation is made for the area, which is used together with the age data to highlight the foreland basin evolution. The palynological part of the paper has been summarized in Pavlishina *et al.* (2008).

2. Geological setting

The Magallanes Basin comprises more than 7,000 m of sedimentary rocks overlying Paleozoic basement. Deposition first occurred during a mechanical graben stage, followed by a thermal subsidence stage and later a series of foreland orogenic loading stages (Biddle *et al.*, 1986). The stratigraphic succession is comprised of a base of Upper Jurassic submarine rhyolites and water-laid tuffs synchronous with the rifting events (Gust *et al.*, 1985; Wilson, 1991). During the subsequent thermal subsidence stage, the synrift units were covered by the subsurface oil-bearing sands of the Springhill Formation and the mainly fine-grained sedimentary rocks of the Beauvoir and equivalent formations (see legend of Fig.1). A minimum age for the strongly folded Beauvoir slates is provided by the doubtful 104±4 Ma whole rock K-Ar age of a spililitic dike (Martinioni *et al.*,

[1] Céspedes, S. 1971. Estudio geológico de la zona de Cabo Nariz y Tierra del Fuego. Empresa Nacional de Petróleo, Informe Técnico (Unpublished): 70 p.

[2] Rojas, L.; Harambour, S.; Robertson, R.; Castelli, J.C. 1993. Geología, geofísica y delimitación de prospectos Bloque Lago Blanco. Empresa Nacional de Petróleo, Informe Técnico (Unpublished): 146 p.

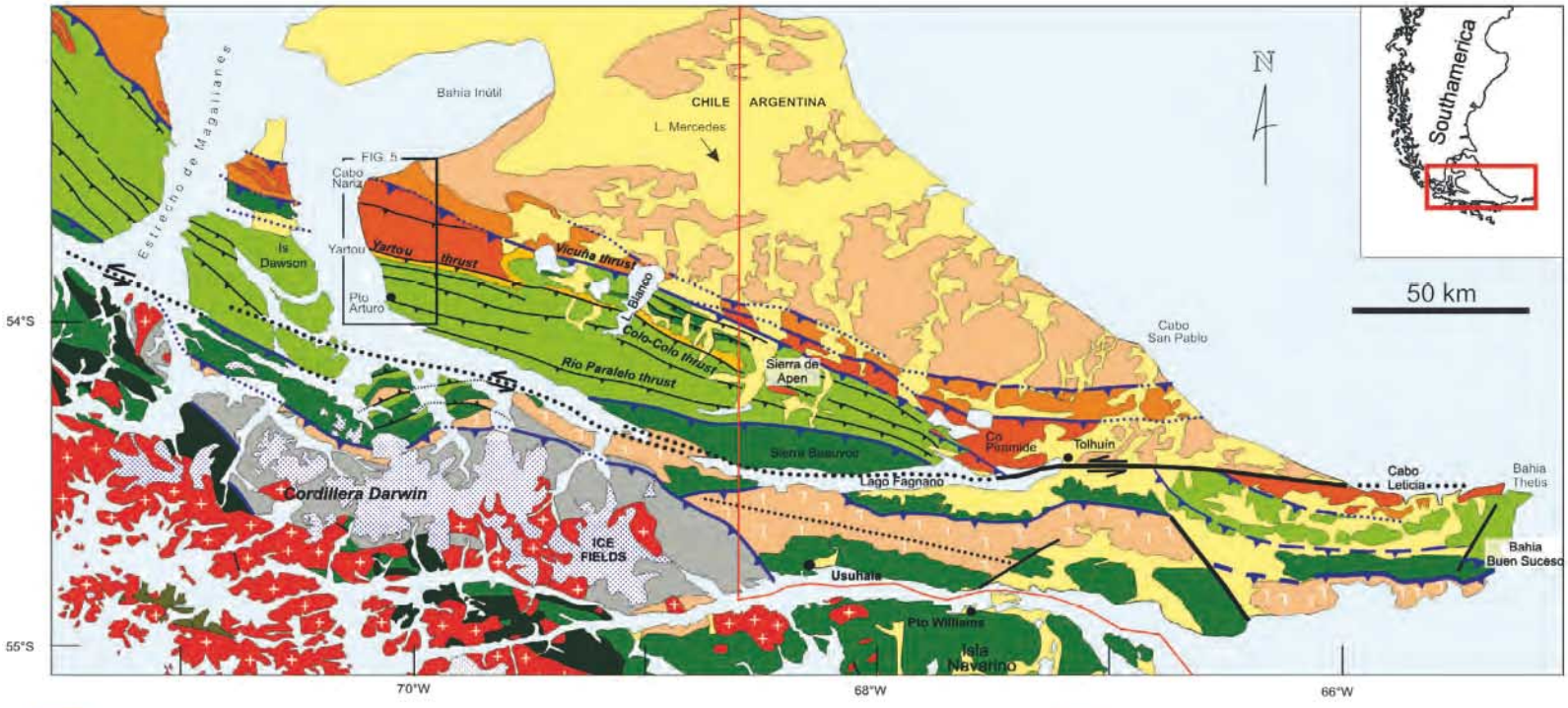

Unconsolidated Quaternary sediments

Oligocene- Miocene foreland sequence

Eocene foreland sequence
(Río Bueno, Río Cóndor, Cabo Leticia, Cerro Colorado Fms.; Ballena Group and equivalent units)

Paleocene- Early Eocene foreland sequence
(Tres Amigos, Chorrillo Chico, Río Claro, Leticia, La Barca, Punta Noguera, Cerro Ruperto, Punta Torcida, Cabo Nariz Fms.)

Late Cretaceous-Danian foreland sequence
Maastrichtian-Danian (Cerro Cuchilla and Policarpo Fms.)
Coniacian -Maastrichtian (Cerro Matrero, Buen Suceso, Bahía Thethis Fms. and equivalent units.
Early Cretaceous arc volcanics (Hardy Fm.)

Early Cretaceous (Neocomian-Turonian) "thermal subsidence" sequence
Beauvoir, Río Jackson, Vicuña, La Paciencia, Yaghan and Río García Fms.

Rocas Verdes Basin Ophiolites (Late Jurassic Early Cretaceous)
Mid-Late Jurassic volcanics (Tobífera and Lemaire Fms.)

South Patagonian Batholith
Seno Año Nuevo Plutonic Group (60 -34 Ma)
Canal Beagle Plutonic Group (100 -80 Ma)
Late Jurassic "Tobífera" granitoids

Cordillera Darwin Metamorphic Complex (Paleozoic protolith with Mid Cretaceous metamorphic overprinting)

FIG. 1. Regional geologic map of Tierra del Fuego, modified from Suárez *et al.* (1985), Mpodozis (2005)[5], Torres Carbonell *et al.* (2008) and Olivero and Malumián (2008). The studied area (inner box) and localities mentioned in the text are shown.

[5] Mpodozis, C. 2005. Mapa geológico generalizado de la Isla Grande de Tierra del Fuego. Empresa Nacional de Petróleo, Informe Técnico (Unpublished): 2 p. Magallanes.

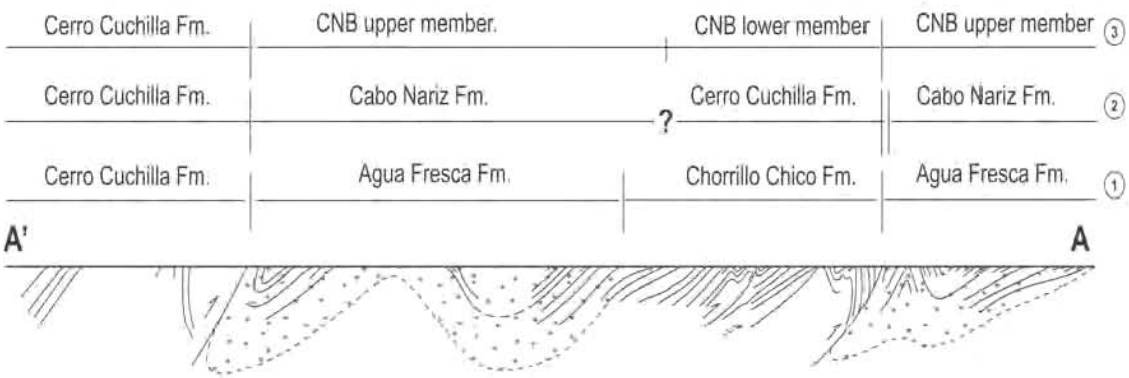

FIG. 2. Profile of Cabo Nariz area sketching the differences between geologic assesment in previous works. 1. Céspedes (1971)[1]; 2. Rojas *et al.* (1993)[2]; 3. This work. Profile after Céspedes (1971)[1].

1999). Lastly, Upper Cretaceous to Miocene turbidites, sandstones and conglomerates fill the basin related to Andean uplift and a consequent flexure subsidence of the basin (Biddle *et al.*, 1986). Furthermore, fold and thrust belt evolution produced a cratonward migration of the basin depocenter (Biddle *et al.*, 1986; Álvarez-Marrón *et al.*, 1993; Rojas and Mpodozis, 2006) (see Fig. 3). Orogenic loading north of this area, at Última Esperanza, started during Turonian times (Fildani *et al.*, 2003), while the Cordillera Darwin uplift is calculated to have started at around 100 Ma (see review *in* Ghiglione and Ramos, 2005).

The sedimentary environments reported in Tierra del Fuego, specifically during the Late Cretaceous-Paleocene transition, can be summarized as follows: during the upper Campanian/Maastrichtian deep submarine channel/levee facies were present at Bahía Thetis Formation in Bahia Buen Suceso area (Olivero *et al.*, 2003), while proximal submarine fan facies (Cerro Matrero Formation) predominate at Seno Almirantazgo (Harambour *et al.*, 1989[4]). Rocks cropping up in the Atlantic coast and Bahía Buen Suceso area, on the other hand, record Maastrichtian/Danian deep submarine fan deltas entering into platform and/or talus environment. They have been included in the Policarpo Formation by Olivero *et al.* (2002) and are equivalent to the Cerro Cuchilla Formation of this study. Finally, in the Argentinean Andes of Tierra del Fuego, all Paleocene rocks record fan delta facies, and from east to west, they are: Tres Amigos Formation (Olivero *et al.*, 2003); Cabo Leticia (Olivero *et al.*, 2002), Cerro Piramide (Olivero and Malumián, 2008) and Sierra de Apen conglomerates (Martinioni *et al.*, 1998). In the Chilean side, Paleocene outcrops are also of fan delta facies, but only near the Argentina/Chile border and representing a progradating system until Eocene (Prieto and Moraga, 1990). To the northwest, submarine fan facies of proximal facies predominate in Cabo Nariz area and distal facies in Isla Riesco and Península Brunswick area (Chorrillo Chico Formation in Rojas *et al.*, 1993[2]).

All these sequences are affected by tectonism of the MFTB until Miocene times (Álvarez-Marrón *et al.*, 1993), and the whole succession changes its principal orientation from north-south at 51°S to a nearly east-west orientation in Tierra del Fuego. This curvature of the sedimentary successions is parallel to the curvature of the main range and to the continental margin.

This paper deals with the foreland sedimentary succession at Cabo Nariz, comprising mainly siltstones with interbedded, slumped sandstones (Fig. 4) of late Campanian to Middle Paleocene age. A more detailed study was undertaken north of the Yartou Thrust (Fig. 5).

3. Methodology

Because the sedimentary succession is a rather cyclic succession of strata that have been affected by tectonism of the MFTB, several techniques were applied to determine the stratigraphy: **1.** measurement of stratigraphic sections, **2.** radiometric dating of detrital zircons and **3.** palynological studies, including age assessment of dinoflagellate cyst assemblages.

[4] Harambour, S.; Urzúa, F.; Aguirre, G. 1989. Evaluación geológica y petrolera Bloque 7, Tierra del Fuego. Empresa Nacional del Petróleo, Informe Técnico (Unpublished): 336 p.

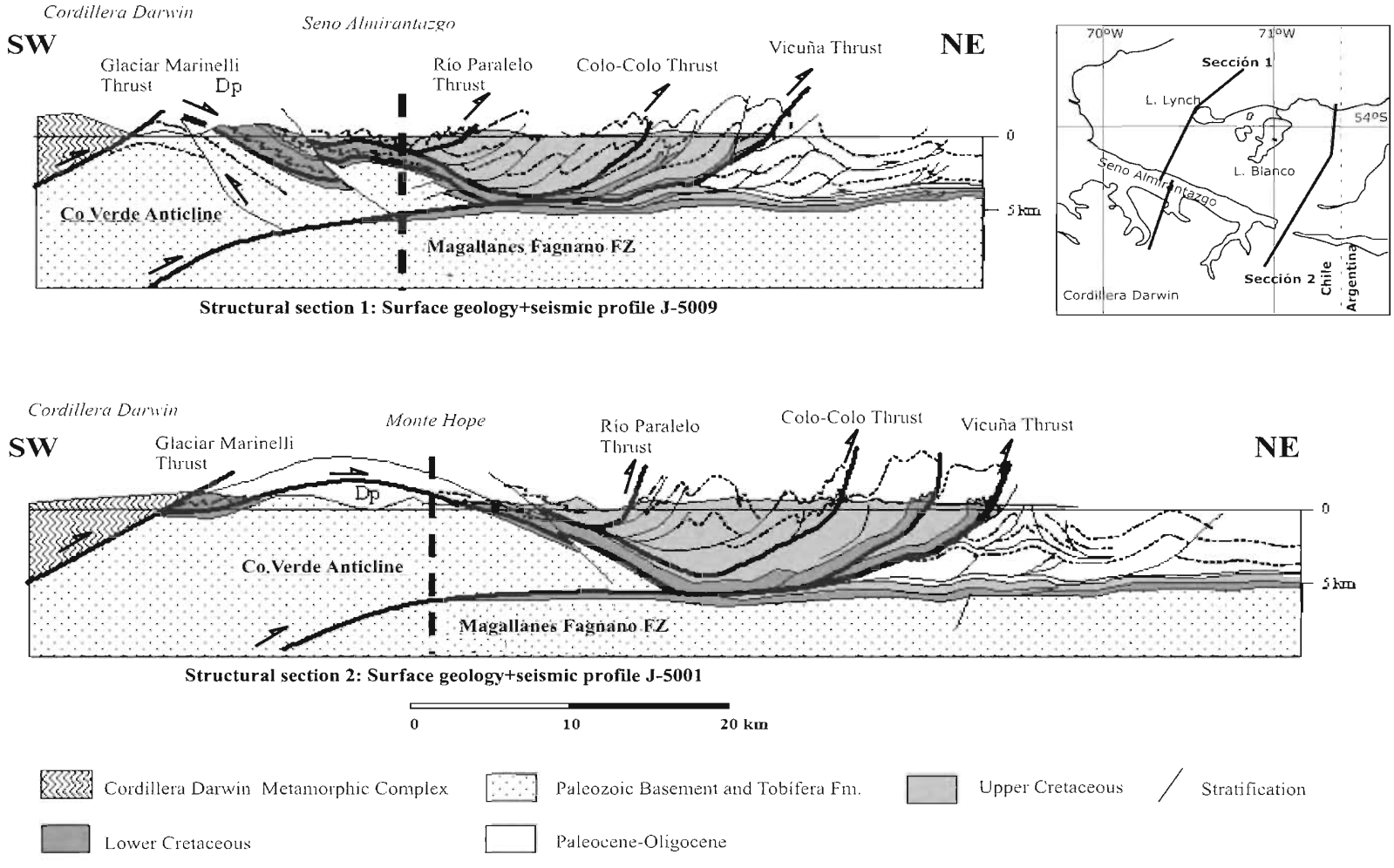

FIG. 3. Tectonic profiles southeast of Cabo Nariz (Rojas and Mpodozis, 2006). The foreland sequence, comprised by Upper Cretaceous and Paleogene units, becomes younger cratonward (NE).

FIG. 4. Outcrops of the Cabo Nariz Beds: 1. Marine terrace with the predominant monotonous Cabo Nariz Beds (CNB); 2. Sandstone clast in the lower member of CNB, facies A; 3. Sandstone concretion with a clast core in the lower member. This interrupts a monotonous succession in facies A. The arrows show ubiquitous sandstone beds; 4. Amalgamation of sandstone beds over siltstones in facies B of the lower member; 5. Paleochannel amalgamation in facies D (upper member). The arrows show rounded intraclasts in the lower channel.

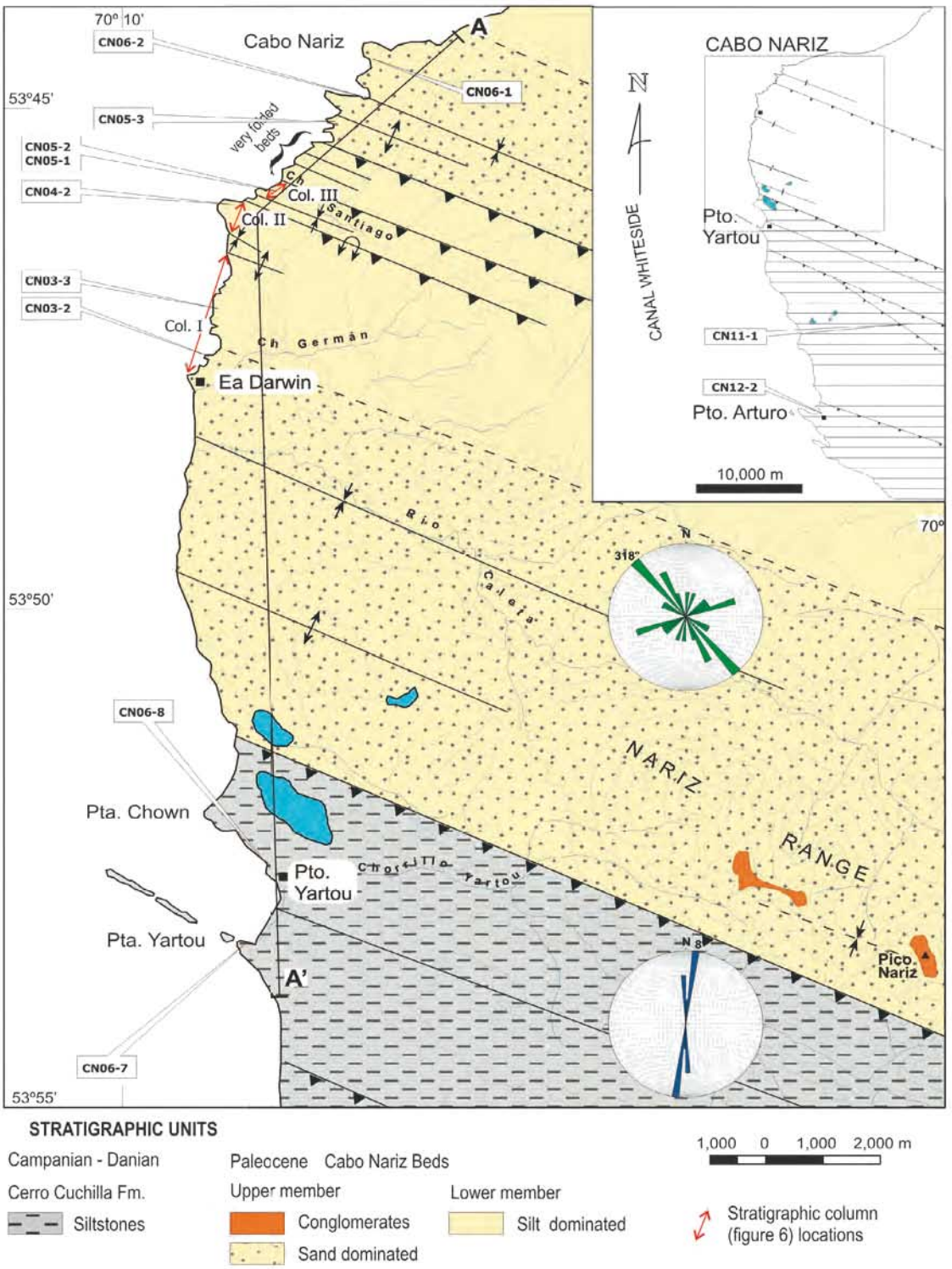

FIG. 5. Geologic map of Cabo Nariz area, showing sample locations, stratigraphic columns of figure 6, and the location of structural profile in figure 9. The rose diagrams illustrate the orientation of sandstone dikes in the CNB (green) and Cerro Cuchilla Formation (blue). Horizontal lined area in the inner box, are Upper Cretaceous sedimentary rocks (Cerro Matrero and Cerro Cuchilla formations); white area corresponds to Cenozoic strata. Geology after Céspedes (1971)[1].

For the palynological studies, siltstone samples collected from the study area (Table 1) were prepared at the Sofia University, Bulgaria, using standard palynological preparation techniques, including HCL, HF treatment, heavy liquid separation and oxidation with HNO_3. Strew mounts were made in glycerine jelly and now are hosted in the collections of the Sofia University 'Saint Kliment Ohridski'. The dinoflagellate cyst taxonomy and nomenclature follows Williams *et al.* (1998) and all citations are fully referenced in their index of fossil genera and species.

Two sedimentary samples (CN05-1 and CN06-1) of the Cabo Nariz Beds were collected for U-Pb zircon dating by SHRIMP RG at The Australian National University, Canberra. The procedures followed are similar to those outlined by Williams (1998). Zircon concentrates were prepared at the Universidad de Chile. In Canberra, representative fractions were strewn on double-sided tape together with the Temora reference zircons and then cast into an epoxy mount. Reflected and transmitted light photomicrographs and cathodoluminescence (CL) scanning electron microscope (SEM) images were prepared for all zircon grains (not shown). The CL images were used to study the internal structures of the sectioned grains and to ensure that the ~20 μm SHRIMP spot was wholly within a single age component for each sectioned grain, avoiding inclusions and zoned crystals. Within each sample, an area was selected at random and 60 grains were analyzed without regard to appearance, in order to minimize bias towards any particular morphological member of the population and to provide valid provenance patterns. The data were reduced using the SQUID Excel Macro of Ludwig (2001). The Pb-U ratios were normalized relative to a value of 0.0668 for the Temora reference zircon, equivalent to an age of 417 Ma (see Black *et al.*, 2003). Uncertainties given for individual analyses (ratios and ages) are at the one sigma level (Tables 2 and 3). Tera and Wasserburg (1972) concordia plots, probability density plots with stacked histograms and weighted mean $^{206}Pb/^{238}U$ age calculations were carried out using ISOPLOT/EX (Ludwig, 2003). The 'Mixture Modelling' algorithm of Sambridge and Compston (1994), via ISOPLOT/EX, was used to un-mix statistical age populations or groupings; from these groups weighted mean $^{206}Pb/^{238}U$ ages were calculated and the uncertainties are reported as 95% confidence limits.

TABLE 1. SAMPLE LOCATION AND THEIR KÜBLER INDEX (KI)

Sample	Rock type	Geographic location	UTM		Formation	KI[a]
			E	N		
CN03-2	siltstone	Ea. Darwin	-	-	Upper CN Beds	0.99
CN03-3	siltstone	Ea. Darwin	423,189	4,039,531	Lower CN Beds	1.03
CN04-2	siltstone	Chorrillo Santiago	423,334	4,041,337	Lower CN Beds	0.77
CN05-1	sandstone	Chorrillo Santiago	423,766	4,041,756	Lower CN Beds	-
CN05-2	siltstone	Chorrillo Santiago	423,766	4,041,756	Lower CN Beds	0.85
CN05-3	siltstone	sur de Cabo Nariz	424,948	4,042,807	Upper CN Beds	1.06
CN06-1	sandstone	Cabo Nariz	425,299	4,044,487	Upper CN Beds	-
CN06-2	siltstone	sur de Cabo Nariz	425,510	4,043,471	Upper CN Beds	1.2
CN06-7	siltstone	Pta. Yartou	424,489	4,027,708	Cerro Cuchilla Fm.	0.97
CN06-8	siltstone	Pto. Yartou	-	-	Cerro Cuchilla Fm.	0.62
CN11-1	siltstone	'camino Trilium'	438,438	4,019,622	Cerro Matrero Fm.	1.12
CN12-2	siltstone	Pto. Arturo	431,617	4,009,142	Cerro Matrero Fm.	0.59

[a]: XRD measured in Departamento de Física de la Universidad de Chile (Sánchez *et al.*, 2005).

TABLE 2. SUMMARY OF SHRIMP U-Pb ZIRCON RESULTS FOR SAMPLE CN05-1.

							Total Ratios				Radiogenic Ratio		Age (Ma)	
Grain spot	U (ppm)	Th (ppm)	Th/U	$^{206}Pb^*$ (ppm)	$^{204}Pb/^{206}Pb$	f_{206} %	$^{238}U/^{206}Pb$	±	$^{207}Pb/^{206}Pb$	±	$^{206}Pb/^{238}U$	±	$^{206}Pb/^{238}U$	±
1.1	471	327	0.70	4.9	0.000502	0.76	82.44	1.29	0.0536	0.0016	0.0120	0.0002	77	1
2.1	755	662	0.88	9.3	0.000200	0.12	69.99	0.90	0.0488	0.0011	0.0143	0.0002	91	1
3.1	265	197	0.74	2.8	0.000696	0.28	82.08	1.54	0.0498	0.0023	0.0121	0.0002	78	1
4.1	464	210	0.45	7.3	0.001008	0.86	54.42	0.83	0.0552	0.0015	0.0182	0.0003	116	2
5.1	819	205	0.25	9.7	0.000549	0.76	72.28	0.95	0.0538	0.0015	0.0137	0.0002	88	1
6.1	2,453	703	0.29	55.8	0.000038	0.02	37.80	0.41	0.0496	0.0005	0.0265	0.0003	168	2
7.1	1,436	334	0.23	14.7	0.000452	1.20	84.15	1.59	0.0570	0.0012	0.0117	0.0002	75	1
8.1	448	110	0.24	5.9	0.000368	0.58	65.16	0.98	0.0526	0.0017	0.0153	0.0002	98	1
9.1	338	372	1.10	6.0	0.000419	1.00	47.96	0.72	0.0566	0.0026	0.0206	0.0003	132	2
10	329	189	0.57	4.8	0.000378	0.41	58.64	0.94	0.0514	0.0019	0.0170	0.0003	109	2
11	528	334	0.63	5.3	0.000317	0.53	85.67	1.28	0.0517	0.0018	0.0116	0.0002	74	1
12	1,173	536	0.46	12.1	0.000096	<0.01	83.36	1.11	0.0473	0.0011	0.0120	0.0002	77	1
13	142	79	0.55	1.8	-	0.84	66.15	1.45	0.0546	0.0040	0.0150	0.0003	96	2
14	1,100	374	0.34	11.3	0.000071	0.07	83.87	1.06	0.0481	0.0011	0.0119	0.0002	76	1
15	540	368	0.68	5.7	0.000298	0.17	80.81	1.22	0.0490	0.0017	0.0124	0.0002	79	1
16	1,529	535	0.35	15.6	0.000147	0.16	84.10	1.00	0.0488	0.0009	0.0119	0.0001	76	1
17	370	281	0.76	4.2	0.000540	0.56	75.59	1.20	0.0521	0.0019	0.0132	0.0002	84	1
18	1,558	322	0.21	15.8	0.000127	0.02	84.83	1.01	0.0477	0.0009	0.0118	0.0001	76	1
19	1,147	366	0.32	11.7	0.000066	-0.07	84.27	1.06	0.0470	0.0011	0.0119	0.0002	76	1
20	981	482	0.49	9.0	0.000186	0.28	94.06	1.31	0.0496	0.0013	0.0106	0.0001	68	1
21	93	67	0.72	1.5	0.000524	0.85	53.44	2.01	0.0551	0.0033	0.0186	0.0007	119	4
22	352	117	0.33	7.4	0.000618	0.48	41.02	0.58	0.0529	0.0014	0.0243	0.0003	155	2
23	315	212	0.67	3.2	0.000730	0.82	83.89	1.47	0.0540	0.0023	0.0118	0.0002	76	1
24	1,134	275	0.24	25.3	-	0.09	38.53	0.44	0.0501	0.0008	0.0259	0.0003	165	2
25	104	137	1.31	8.1	-	<0.01	11.02	0.17	0.0585	0.0015	0.0908	0.0015	560	9
26	1,068	632	0.59	23.2	-	0.18	39.51	0.46	0.0507	0.0008	0.0253	0.0003	161	2
27	890	557	0.63	9.2	0.000270	0.36	82.87	1.10	0.0504	0.0013	0.0120	0.0002	77	1
28	333	134	0.40	7.1	0.000163	0.36	40.46	0.59	0.0521	0.0015	0.0246	0.0004	157	2
29	364	147	0.40	4.5	0.000441	0.42	69.94	1.15	0.0511	0.0020	0.0142	0.0002	91	2
30	280	143	0.51	3.0	0.001256	0.64	81.15	1.48	0.0526	0.0025	0.0122	0.0002	78	1
31	614	537	0.88	6.3	0.000163	0.27	83.17	1.22	0.0497	0.0016	0.0120	0.0002	77	1
32	434	166	0.38	4.5	0.002430	3.80	83.25	1.47	0.0776	0.0100	0.0116	0.0003	74	2
33	413	216	0.52	4.8	0.000310	0.33	74.44	1.17	0.0504	0.0018	0.0134	0.0002	86	1
34	1,509	715	0.47	15.8	0.000244	0.43	82.18	0.98	0.0510	0.0010	0.0121	0.0001	78	1
35	650	461	0.71	6.6	0.000313	0.17	84.64	1.20	0.0489	0.0015	0.0118	0.0002	76	1
36	546	366	0.67	5.6	0.000520	0.41	83.67	1.28	0.0508	0.0018	0.0119	0.0002	76	1
37	312	191	0.61	3.0	0.001219	0.23	88.06	1.59	0.0493	0.0022	0.0113	0.0002	73	1
38	235	258	1.10	3.5	0.000376	0.50	58.21	1.04	0.0522	0.0023	0.0171	0.0003	109	2
39	1,823	460	0.25	17.6	-	0.19	89.08	1.08	0.0489	0.0010	0.0112	0.0001	72	1
40	321	160	0.50	2.9	0.000068	0.08	96.45	1.73	0.0480	0.0030	0.0104	0.0002	66	1
41	199	198	0.99	3.5	0.000961	0.30	48.35	0.84	0.0511	0.0021	0.0206	0.0004	132	2
42	464	260	0.56	5.3	0.000261	0.16	74.88	1.22	0.0490	0.0016	0.0133	0.0002	85	1
43	65	35	0.55	1.0	-	2.56	57.95	1.64	0.0685	0.0048	0.0168	0.0005	107	3
44	147	91	0.62	2.6	-	0.48	49.04	0.94	0.0525	0.0024	0.0203	0.0004	130	2
45	386	280	0.72	4.0	-	<0.01	83.07	1.35	0.0475	0.0019	0.0120	0.0002	77	1
46	455	357	0.78	4.8	-	0.03	80.89	1.27	0.0478	0.0018	0.0124	0.0002	79	1
47	688	598	0.87	7.0	0.000351	0.24	84.12	1.74	0.0494	0.0014	0.0119	0.0002	76	2
48	240	154	0.64	2.8	0.000551	0.65	73.02	1.39	0.0529	0.0025	0.0136	0.0003	87	2
49	1,513	351	0.23	15.6	0.000265	0.34	83.50	1.00	0.0502	0.0010	0.0119	0.0001	76	1

Table 2. continued.

Grain spot	U (ppm)	Th (ppm)	Th/U	$^{206}Pb^*$ (ppm)	$^{204}Pb/^{206}Pb$	f_{206} %	Total Ratios $^{238}U/^{206}Pb$	±	$^{207}Pb/^{206}Pb$	±	Radiogenic Ratio $^{206}Pb/^{238}U$	±	Age (Ma) $^{206}Pb/^{238}U$	±
50	389	235	0.60	4.0	0.000901	0.34	84.40	1.39	0.0503	0.0020	0.0118	0.0002	76	1
51	796	50	0.06	6.6	0.000119	0.37	103.87	1.47	0.0502	0.0015	0.0096	0.0001	62	1
52	241	61	0.26	13.1	0.000169	0.47	15.79	0.21	0.0583	0.0012	0.0630	0.0009	394	5
53	712	274	0.38	8.2	0.000100	<0.01	74.24	1.01	0.0471	0.0013	0.0135	0.0002	86	1
54	1,138	425	0.37	11.8	0.000197	<0.01	82.90	1.04	0.0474	0.0011	0.0121	0.0002	77	1
55	449	356	0.79	4.6	0.001039	1.90	84.69	1.32	0.0626	0.0031	0.0116	0.0002	74	1
56	270	131	0.48	3.5	0.001048	0.86	66.95	1.16	0.0547	0.0022	0.0148	0.0003	95	2
57	127	58	0.46	1.8	0.000073	0.15	58.82	1.51	0.0494	0.0035	0.0170	0.0004	109	3
58	249	110	0.44	3.0	0.000394	0.29	71.37	1.32	0.0501	0.0023	0.0140	0.0003	89	2
59	360	249	0.69	4.2	0.000436	<0.01	73.75	1.18	0.0465	0.0018	0.0136	0.0002	87	1
60	563	231	0.41	6.5	0.000324	0.34	74.54	1.06	0.0504	0.0015	0.0134	0.0002	86	1

Notes: 1. Uncertainties given at the one σ level; **2.** Error in Temora reference zircon calibration was 0.70% for the analytical session (not included in above errors but required when comparing data from different mounts); **3.** f_{206} % denotes the percentage of ^{206}Pb that is common Pb.; **4.** Correction for common Pb made using the measured $^{238}U/^{206}Pb$ and $^{207}Pb/^{206}Pb$ ratios following Tera and Wasserburg (1972) as outlined in Williams (1998).

A maximum age for the deposition of the host rock sample may be determined from the weighted mean age of the youngest significant age peak in these distributions, that is where there are ≥3 analyses within analytical uncertainty. Such an age grouping takes into account isolated cases of Pb-loss which can produce minor scatter to younger ages.

4. Stratigraphy and sedimentology

Based on three stratigraphic sections measured between Estancia Darwin and Chorrillo Santiago (Figs. 5 and 6), several facies assemblages were recognised. Siltstones with interbedded sandstones, siltstone-rich turbidites, amalgamated sandstones, sandstones with intraformational conglomerates and conglomerates predominate. The data we present here have been used to propose a new definition of units for the sedimentary successions outcropping in the area.

4.1. Cerro Cuchilla Formation (Upper Campanian-Lower Danian)

This formation that crops out south of Punta Chown (Fig. 5) is comprised of up to 420 m of thick-bedded siltstones with intercalated marls. Coarse-grained turbidite sandstones up to 50 cm thick also occur sporadically within the succession (Céspedes, 1971)[1]. The base and top of the formation are not exposed.

4.1.1. Lithology

The siltstone beds, dark grey to black in outcrop, are 5 to 50 cm thick and have a low calcareous content. At Punta Yartou they host many calcareous concretions of 5 to 15 cm in diameter, and they have frequent intercalations of centimeter-scale marl beds. The sandstones, mainly yellow to green lithic wackes, occur as rare 20 to 50 cm thick intercalations in the siltstones. They have between 10 and 30% of calcareous matrix.

4.1.2. Facies interpretation

The siltstones are interpreted to have been deposited in quiet environment out of wave action in slope or platform environment. The wide continuity of centimetric-scale sandstone intercalations may represent deposits of turbidity current, which spread out of the slope, probably triggered by seismic activity.

4.2. Cabo Nariz Beds (Selandian-Thanetian)

Over 1,500 m of turbidites, subdivided in two members, crop out between Cabo Nariz and Estancia Darwin, discontinuously south of the latter (Fig. 5). They are structurally below the Cerro Cuchilla Formation. Neither the top nor the bottom of this succession crops out in the study area. The beds are divided into a lower and upper member with 5 facies assemblages.

4.2.1. Lower Member

The lower member includes two alternating facies assemblages: the *siltstone and minor sand-*

TABLE 3. SUMMARY OF SHRIMP U-Pb ZIRCON RESULTS FOR SAMPLE CN06-1.

							Total Ratios				Radiogenic Ratios							Age (Ma)				
Grain spot	U (ppm)	Th (ppm)	Th/U	$^{206}Pb^*$ (ppm)	$^{204}Pb/^{206}Pb$	f_{206} %	$^{238}U/^{206}Pb$	±	$^{207}Pb/^{206}Pb$	±	$^{206}Pb/^{238}U$	±	$^{207}Pb/^{235}U$	±	$^{207}Pb/^{206}Pb$	±	ρ	$^{206}Pb/^{238}U$	±	$^{207}Pb/^{206}Pb$	±	% Disc
1.1	377	346	0.92	8.2	0.000163	0.43	39.47	0.55	0.0527	0.0014	0.0252	0.0004	-	-	-	-	-	161	2	-	-	-
2.1	164	115	0.70	1.7	-	0.68	82.78	1.83	0.0530	0.0031	0.0120	0.0003	-	-	-	-	-	77	2	-	-	-
3.1	1,588	472	0.30	16.3	0.000047	0.15	83.75	0.99	0.0487	0.0009	0.0119	0.0001	-	-	-	-	-	76	1	-	-	-
4.1	529	400	0.76	5.6	0.000591	0.60	81.33	1.33	0.0523	0.0017	0.0122	0.0002	-	-	-	-	-	78	1	-	-	-
5.1	183	140	0.77	27.8	-	<0.01	5.66	0.07	0.0744	0.0009	0.1768	0.0022	1,818	0.033	0.0746	0.0010	0.701	1,050	12	1,057	26	1
6.1	100	46	0.46	1.4	0.000576	0.49	59.49	1.46	0.0520	0.0034	0.0167	0.0004	-	-	-	-	-	107	3	-	-	-
7.1	977	899	0.92	7.7	0.000444	0.18	108.69	1.59	0.0486	0.0014	0.0092	0.0001	-	-	-	-	-	59	1	-	-	-
8.1	164	90	0.55	2.4	0.000548	0.46	59.11	1.18	0.0519	0.0026	0.0168	0.0003	-	-	-	-	-	108	2	-	-	-
9.1	572	355	0.62	8.5	0.000190	0.10	58.02	0.79	0.0490	0.0013	0.0172	0.0002	-	-	-	-	-	110	2	-	-	-
10	311	108	0.35	4.0	0.000284	0.24	67.34	1.09	0.0498	0.0019	0.0148	0.0002	-	-	-	-	-	95	2	-	-	-
11	274	165	0.60	2.8	-	0.27	84.06	1.60	0.0496	0.0024	0.0119	0.0002	-	-	-	-	-	76	1	-	-	-
12	379	241	0.64	4.6	-	0.41	70.58	1.11	0.0510	0.0018	0.0141	0.0002	-	-	-	-	-	90	1	-	-	-
13	558	248	0.45	5.3	0.000179	0.28	89.61	1.51	0.0496	0.0019	0.0111	0.0002	-	-	-	-	-	71	1	-	-	-
14	123	95	0.78	2.1	0.045582	51.74	49.63	1.28	0.4576	0.0131	0.0097	0.0005	-	-	-	-	-	62	3	-	-	-
15	409	224	0.55	3.3	0.002614	2.75	106.70	1.95	0.0689	0.0041	0.0091	0.0002	-	-	-	-	-	58	1	-	-	-
16	262	171	0.66	3.7	0.000107	0.05	60.30	1.03	0.0486	0.0020	0.0166	0.0003	-	-	-	-	-	106	2	-	-	-
17	446	109	0.24	4.6	0.000238	0.28	83.61	1.31	0.0498	0.0018	0.0119	0.0002	-	-	-	-	-	76	1	-	-	-
18	34	16	0.47	0.5	0.003888	0.69	58.32	2.25	0.0537	0.0057	0.0170	0.0007	-	-	-	-	-	109	4	-	-	-
19	236	125	0.53	2.7	0.000794	0.05	74.97	1.40	0.0481	0.0023	0.0133	0.0003	-	-	-	-	-	85	2	-	-	-
20	85	72	0.84	12.6	0.000127	0.22	5.82	0.09	0.0744	0.0014	0.1715	0.0026	1,717	0.048	0.0726	0.0017	0.549	1,020	14	1,003	47	-2
21	1,667	814	0.49	16.0	0.000627	0.36	89.37	1.16	0.0503	0.0015	0.0111	0.0001	-	-	-	-	-	71	1	-	-	-
22	1,269	1,160	0.91	15.7	0.000110	0.14	69.66	0.96	0.0490	0.0016	0.0143	0.0002	-	-	-	-	-	92	1	-	-	-
23	2,235	1,624	0.73	26.6	-	0.05	72.14	0.85	0.0482	0.0011	0.0139	0.0002	-	-	-	-	-	89	1	-	-	-
24	129	60	0.47	1.8	-	1.25	62.43	1.60	0.0580	0.0045	0.0158	0.0004	-	-	-	-	-	101	3	-	-	-
25	2,018	1,648	0.82	15.7	0.000359	<0.01	110.62	1.41	0.0437	0.0013	0.0091	0.0001	-	-	-	-	-	58	1	-	-	-
26	2,941	684	0.23	29.1	0.000392	0.02	86.73	1.02	0.0477	0.0015	0.0115	0.0001	-	-	-	-	-	74	1	-	-	-
27	1,118	855	0.76	8.4	0.000566	<0.01	114.48	2.40	0.0462	0.0019	0.0087	0.0002	-	-	-	-	-	56	1	-	-	-
28	1,048	808	0.77	8.2	0.000420	<0.01	110.10	1.62	0.0449	0.0034	0.0091	0.0001	-	-	-	-	-	58	1	-	-	-
29	453	153	0.34	4.5	-	0.01	86.35	1.56	0.0476	0.0027	0.0116	0.0002	-	-	-	-	-	74	1	-	-	-
30	79	34	0.42	1.1	0.001676	2.08	63.49	2.10	0.0645	0.0063	0.0154	0.0005	-	-	-	-	-	99	3	-	-	-
31	410	173	0.42	3.2	0.003110	0.31	111.26	2.50	0.0496	0.0031	0.0090	0.0002	-	-	-	-	-	58	1	-	-	-
32	587	323	0.55	5.9	0.000481	<0.01	84.95	1.53	0.0472	0.0023	0.0118	0.0002	-	-	-	-	-	75	1	-	-	-
33	2,030	2,238	1.10	15.2	0.000237	0.17	114.40	1.48	0.0485	0.0015	0.0087	0.0001	-	-	-	-	-	56	1	-	-	-

Table 3. continued.

							Total Ratios				Radiogenic Ratios							Age (Ma)				
Grain	U	Th	Th/U	$^{206}Pb^*$	$^{204}Pb/$	f_{206}	$^{238}U/$		$^{207}Pb/$		$^{206}Pb/$		$^{207}Pb/$		$^{207}Pb/$			$^{206}Pb/$		$^{207}Pb/$		%
spot	(ppm)	(ppm)		(ppm)	^{206}Pb	%	^{206}Pb	±	^{206}Pb	±	^{238}U	±	^{235}U	±	^{206}Pb	±	ρ	^{238}U	±	^{206}Pb	±	Disc
34	1,503	1,407	0.94	11.4	0.000629	0.19	112.84	1.53	0.0486	0.0016	0.0088	0.0001	-	-	-	-	-	57	1	-	-	-
35	755	389	0.52	7.5	0.000238	<0.01	86.65	1.33	0.0474	0.0020	0.0115	0.0002	-	-	-	-	-	74	1	-	-	-
36	495	33	0.07	41.8	0.000073	<0.01	10.17	0.13	0.0574	0.0011	0.0986	0.0012	-	-	-	-	-	606	7	-	-	-
37	543	442	0.81	4.1	0.001755	0.80	113.65	2.07	0.0535	0.0029	0.0087	0.0002	-	-	-	-	-	56	1	-	-	-
38	415	213	0.51	5.4	0.000327	0.07	66.37	1.14	0.0485	0.0024	0.0151	0.0003	-	-	-	-	-	96	2	-	-	-
39	371	222	0.60	5.3	-	<0.01	59.82	1.05	0.0469	0.0024	0.0167	0.0003	-	-	-	-	-	107	2	-	-	-
40	2,749	481	0.17	27.0	0.000196	0.07	87.59	1.03	0.0481	0.0011	0.0114	0.0001	-	-	-	-	-	73	1	-	-	-
41	430	230	0.53	3.3	0.001423	0.42	111.49	2.19	0.0505	0.0031	0.0089	0.0002	-	-	-	-	-	57	1	-	-	-
42	2,044	574	0.28	20.4	0.000178	<0.01	85.93	1.05	0.0453	0.0012	0.0117	0.0001	-	-	-	-	-	75	1	-	-	-
43	614	252	0.41	8.3	0.000275	<0.01	63.22	0.94	0.0480	0.0019	0.0158	0.0002	-	-	-	-	-	101	2	-	-	-
44	2,350	857	0.36	23.3	0.000065	<0.01	86.69	1.04	0.0444	0.0011	0.0116	0.0001	-	-	-	-	-	74	1	-	-	-
45	2,633	569	0.22	26.0	0.000755	0.26	87.16	1.03	0.0495	0.0011	0.0114	0.0001	-	-	-	-	-	73	1	-	-	-
46	362	186	0.51	5.1	0.001405	0.29	61.55	1.08	0.0504	0.0025	0.0162	0.0003	-	-	-	-	-	104	2	-	-	-
47	738	266	0.36	7.4	0.000940	<0.01	85.49	1.31	0.0454	0.0020	0.0117	0.0002	-	-	-	-	-	75	1	-	-	-
48	569	530	0.93	5.8	0.000538	0.21	84.12	1.39	0.0492	0.0023	0.0119	0.0002	-	-	-	-	-	76	1	-	-	-
49	3,045	875	0.29	38.4	0.000230	<0.01	68.07	0.81	0.0472	0.0011	0.0147	0.0002	-	-	-	-	-	94	1	-	-	-
50	179	91	0.51	2.5	0.004069	0.55	62.04	1.41	0.0524	0.0036	0.0160	0.0004	-	-	-	-	-	103	2	-	-	-
51	452	211	0.47	3.6	0.002772	<0.01	108.10	2.08	0.0436	0.0027	0.0093	0.0002	-	-	-	-	-	60	1	-	-	-
52	713	434	0.61	8.8	0.000574	0.15	69.74	1.03	0.0490	0.0019	0.0143	0.0002	-	-	-	-	-	92	1	-	-	-
53	495	361	0.73	5.3	0.000904	<0.01	79.90	1.35	0.0432	0.0023	0.0126	0.0002	-	-	-	-	-	81	1	-	-	-
54	1,774	266	0.15	22.7	0.000325	<0.01	67.11	0.81	0.0478	0.0019	0.0149	0.0002	-	-	-	-	-	95	1	-	-	-
55	723	398	0.55	10.2	0.000262	<0.01	60.84	0.86	0.0455	0.0017	0.0165	0.0002	-	-	-	-	-	105	2	-	-	-
56	1,110	630	0.57	13.1	0.000260	<0.01	72.54	0.97	0.0449	0.0015	0.0138	0.0002	-	-	-	-	-	89	1	-	-	-
57	3,211	1,026	0.32	31.8	-	<0.01	86.63	0.99	0.0450	0.0011	0.0116	0.0001	-	-	-	-	-	74	1	-	-	-
58	1,062	1,318	1.24	10.9	0.000000	<0.01	83.52	1.16	0.0429	0.0016	0.0120	0.0002	-	-	-	-	-	77	1	-	-	-
59	167	84	0.51	1.3	0.004657	2.58	106.54	3.10	0.0676	0.0060	0.0091	0.0003	-	-	-	-	-	59	2	-	-	-
60	845	269	0.32	10.9	-	<0.01	66.71	0.93	0.0466	0.0019	0.0150	0.0002	-	-	-	-	-	96	1	-	-	-

Notes: **1**. Uncertainties given at the one σ level; **2**. Error in Temora reference zircon calibration was 0.70% and 0.67% for the analytical sessions (not included in above errors but required when comparing $^{206}Pb/^{238}U$ data from different mounts); **3**. f_{206} % denotes the percentage of ^{206}Pb that is common Pb; **4**. For areas older than ~800 Ma correction for common Pb made using the measured $^{204}Pb/^{206}Pb$ ratio; **5**. For areas younger than ~800 Ma correction for common Pb made using the measured $^{238}U/^{206}Pb$ and $^{207}Pb/^{206}Pb$ ratios following Tera and Wasserburg (1972) as outlined in Williams (1998); **6**. For % Disc. 0% denotes a concordant analysis.

stone facies (A) consists of 5 to 60 cm thick grey siltstone beds that include rare but very continuous 5 to 15 cm thick, laminated lithic to arkosic wackes with convolute bedding and sandstone clasts that may exceed 1 m in diameter (Figs. 4.2 and 4.3). Groove casts in paleochannels are oriented north-south, while flute casts indicate a NNW sense of transport. Carbonate and rare pyrite concretions are present, as well as echinoderm plates. *The siltstone-rich turbiditic facies* (B) comprises large clast-turbidites, usually with a 5 to 50 cm thick massive to convolute-bedded sandstone base and a siltstone top. The sandstones are lithic-feldspatic wackes with a reduced carbonate matrix. Amalgamation is found both within the sandstones as well as in the paleochannels (Fig. 4.4).

4.2.2. Upper Member

Three facies assemblages are included in the upper member. The *normal-graded sandstone facies* (C) comprises 0.6 to 1 m thick turbidites comprising a massive wacke base, usually with graded bedding, followed by a horizontally laminated sandstone and a siltstone top. *The massive sandstone intraclast-conglomerate* (D) includes lithic wackes up to 2 m thick, pebbly sandstones and conglomerates of variable thickness with rounded sandstones intraclasts up to 1 m in diameter (Fig. 4.5). The wackes, when not amalgamated, are characterized by massive bases with load casts and rare thin siltstone layers. *The polymictic conglomerates* (E) are found in small outcrops of just few square meters near the coastal terrace at Estancia Darwin where thickness cannot be measured, while conglomerates at least 5 m thick crops out in the crest of Cordillera Nariz, in the easternmost part of the studied area. Of the two levels that could be reached, both of undetermined thickness, the lower is a poorly sorted, matrix-supported conglomerate in which clasts are subrounded, slightly spherical, under 5 cm in diameter and the matrix is coarse sandstone. The upper level coarse clast-supported conglomerates make up the higher outcrops in the range.

Facies C is the most common in the lowest part of this member, while transitionally to the top, facies D predominates with rare facies E intercalations.

4.2.3. Facies interpretation and correlation

This formation shows a coarsening-upward pattern which is noted in the predominance of sandy facies in the upper member, whereas the lower member by comparison has more siltstone facies. Within this coarsening pattern, facies A is interpreted as deposited in a deep water marine environment, fed by turbidity currents probably triggered by seismic activity. Facies B is interpreted to be part of a distal submarine fan, which prograded over facies A. The upper member facies are interpreted to reflect a slope environment with proximal fan intercalations (facies C) and interrupted by distributary channels of the fan system (facies D) which are common at the top of the sequence. This fan system prograded north to northwest as revealed by channel orientations, tool marks and flute casts. The conglomerates (facies E) are interpreted as part of a canyon which may have fed the fan system.

5. Fossil content and age

5.1. Cerro Cuchilla Formation

According to Cañón (*in* Céspedes, 1971)[1] at Punta Yartou abundant limestone nodules contain *Baculites ovatus* var. *platisima*, *Maorites* sp., *Neophylloceras ramosum* (Meek, 1857), *Kosmaticeras* sp. and equinoids. We failed to find any invertebrates in this formation. However, two of the samples investigated from this formation (CN06-7 and CN06-8) proved to contain dinoflagellate cysts (Table 4, Fig. 7). The following species were encountered in the assemblage: *Isabelidinium cooksoniae* (Alberti, 1959) Lentin and Williams, 1977; *Isabelidinium majae* Schioler, 1993; *Hystrichosphaeridium salpingophorum* Deflandre, 1935; *Phelodinium magnificum* (Stanley, 1965) Stover and Evitt, 1978; *Phelodinium kozlowskii* (Gorka, 1963) Lindrgen, 1984; *Achomosphaera ramulifera* (Deflandre, 1937) Evitt, 1963; *Spinidinium* spp.; *Palaeocystodinium denticulatum* Alberti, 1961; *Palaeocystodinium* spp.; *Senegalidinium obscura* (Drugg, 1967) Williams *et al.*, 1998; *Deflandrea galeata* (Lejeune-Carpentier, 1942) Lentin and Williams, 1973.

The dinoflagellate assemblage suggests a late Campanian to early Danian age, based on the concurrent range of *Isabelidinium cooksoniae*, *Isabelidinium majae*, *Deflandrea galeata*, *Deflandrea obscura* and *Palaeocystodinium* spp. The first world-wide occurrence of the *Palaeocystodinium* genus is documented in the late Campanian (Williams and Bujak, 1985), so the formation could not be older than this stratigraphic interval.

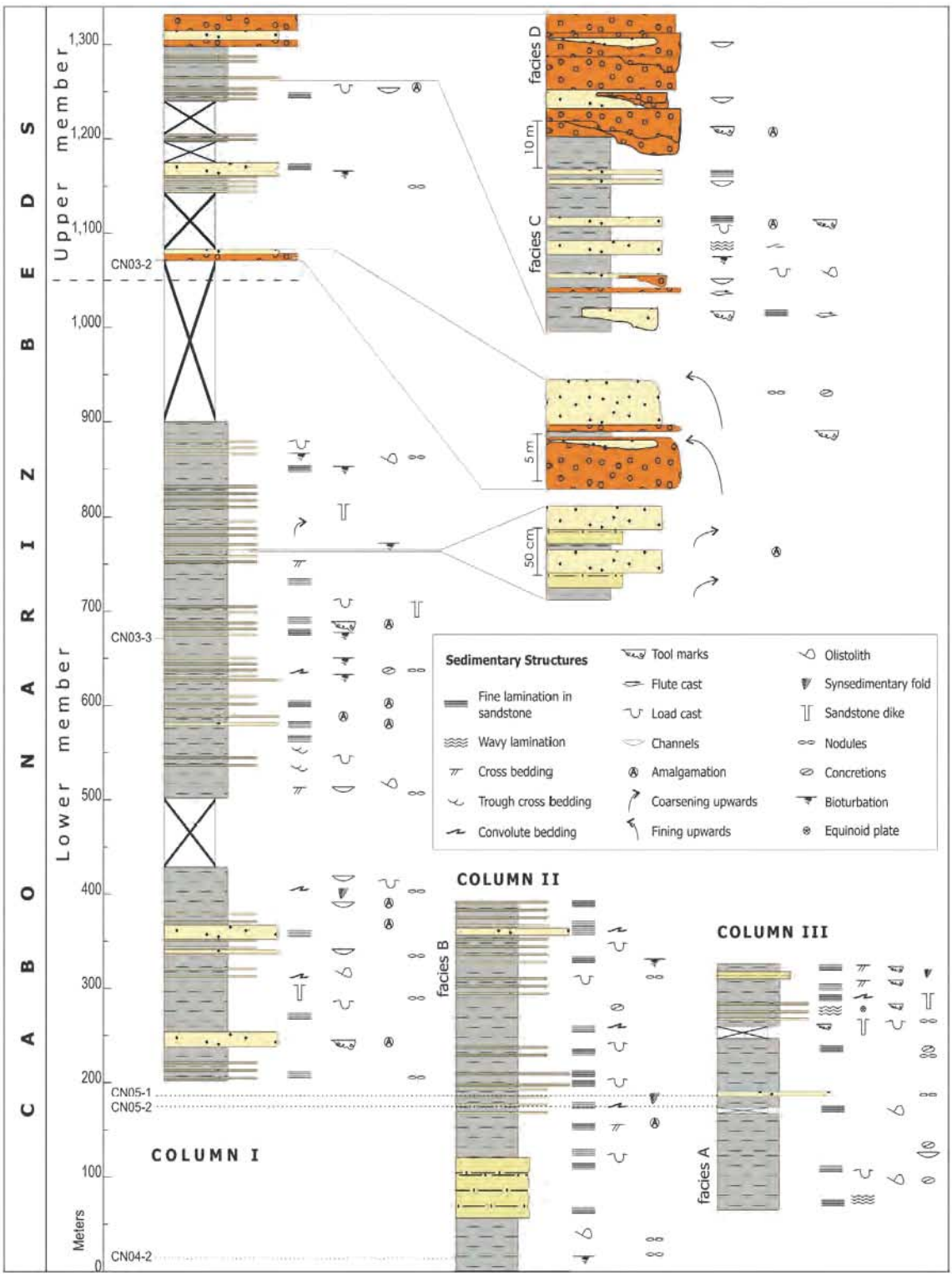

FIG. 6. Stratigraphic columns in Cabo Nariz Beds, north of Estancia Darwin. Location indicated in figure 5. The different sedimentary facies are indicated in the stratigraphic horizons in which they are better developed, symbols can be traced through the column.

5.2. Cabo Nariz Beds

In two samples from the lower member (CN05-2 and CN04-2) the following dinocyst species were recognized: *Hafniasphaera septata* (Cookson and Eisenack, 1967) Hansen, 1977; *Cerodinium depressa* (Morgenroth, 1966) Lentin and Williams, 1977; *Palaeocystodinium lidiae* (Gorka, 1963) Davey, 1969; *Impagidinium* spp.; *Hystrichosphaeridium salpingophorum* Deflandre, 1935; *Cerodinium speciosum* (Alberti, 1959) Lentin and Williams, 1975; *Palaeocystodinium denticulatum* Alberti, 1961 (Table 4, Fig. 7). Based on the concurrent range of the species *Palaeocystodinium lidiae* (Gorka, 1963) Davey, 1969; *Cerodinium depressa* (Morgenroth, 1966) Lentin and Williams, 1977 and *Cerodinium speciosum* (Alberti, 1959) Lentin and Williams, 1975, whose first occurrence and range is documented in the Selandian (Stover *et al.*, 1996), the age of these samples is here specified as Middle Paleocene.

The only productive sample from the upper member is CN06-2. The dinocyst species diversity is low and all encountered specimens belong to three dinocyst species: *Palaeocystodinium australinum* (Cookson, 1965) Lentin and Williams, 1976; *Palaeocystodinium golzowense* Alberti, 1961; *Deflandrea* spp. Their first occurrence is documented world-wide in the middle Paleocene (Selandian) (Williams and Bujak, 1985), so they cannot be older than this stratigraphic interval. Although characteristic, the encountered dinocyst taxa are not sufficient for a more detailed subdivision of this stratigraphic interval.

5.3. Chronostratigraphic correlation

Seventy meters of late Campanian-early Maastrichtian *Calculites obscurus* and *Biscutum dissimilis*-bearing rocks have been described in a 3,400 m deep borehole at Lago Mercedes, close to the border with Argentina. They were assigned to agglutinated foraminifera of a shallow water-lagoon environment, following Malumián and Masiuk (1976). The upper Maastrichtian is missing at this locality because the overlying sandstones carry *Toweius africanus Perch-Nielsen* and are Danian in age (GEMA, 2005)[5]. On the other hand, over 3,000 m of *Heterohelix globulosa* (Ehrenberg)-bearing Maastrichtian turbidites that pinch out eastward (the Rocallosa or Dorotea formations) crop out north of the study area, at Isla Riesco (52°40'S) (Natland *et al.*, 1974).

Neochiastozygus distentus has been recognised together with *Toweius africanus* in 45 m of Paleocene sediments at Lago Mercedes (Fig. 1) (GEMA, 2005)[5]. On the other hand, *Spiroplectammina grzybowskii* Frizzell, *Anomalina rubiginosa* Cushman, *Gyroidina infrafosa* Finlay *and Epistominella texana* Cushman are reported from the top of the 700 m thick Chorrillo Chico Formation, overlying the Danian at Isla Riesco (Natland *et al.*, 1974).

Paleocystodinium golzowense Alberti, 1961 has also been reported along strike east of the national border, in Argentina. Although it has been used here to assign sandstones and conglomerates of the Sierra de Apen (Fig. 1), as well as rocks from the Policarpo formations to the Early Paleocene (Martinioni *et al.*, 1999; Olivero *et al.*, 2003), it has also been documented in La Barca formation assigned to the late Paleocene (Olivero *et al.*, 2002) as has been considered in this work.

5.4. U-Pb dating of Cabo Nariz Beds

Detrital zircons from one sample in each member of the Cabo Nariz Beds were dated using SHRIMP U-Pb. (Fig. 8). Gradstein *et al.* (2004) is used as a chrono-stratigraphic reference.

5.4.1. Lower Member

The detrital zircons from sample CN05-1 are mostly euhedral crystals that in section can be seen to be simple zoned igneous zircon. From the 60 grains analysed there is a dominant peak of 25 grains that have a weighted mean $^{206}Pb/^{238}U$ age of 76.5±0.7 Ma. A subordinate age peak occurs at 86.4±1.1 Ma (9 grains) with scattered older ages ranging up to about 560 Ma. Three of the grains analysed are younger than the dominant 76.5 Ma age peak (Fig. 8). These analyses are low in common Pb and plot close to the Tera-Wasserburg Concordia curve. Two grains have $^{206}Pb/^{238}U$ ages of 66 and 68 Ma respectively (Table 3) whilst grain 51 is the youngest at 62 Ma. A single U-Pb zircon analysis cannot constrain the time of deposition of this sediment. Rather the maximum time of deposition is given by the dominant 76.5±0.7 Ma date for simple zoned igneous zircon grains.

5.4.2. Upper Member

For the sample CN06-1 the zircon grains are seen under CL imaging to be mostly simple zoned igneous crystals. The $^{206}Pb/^{238}U$ ages range from

[5] GEMA, S.R.L. 2005. Análisis bioestratigráfico del pozo Lago Mercedes-1, de la Cuenca de Magallanes, Chile. Empresa Nacional del Petróleo. Informe Técnico (Unpublished): 14 p.

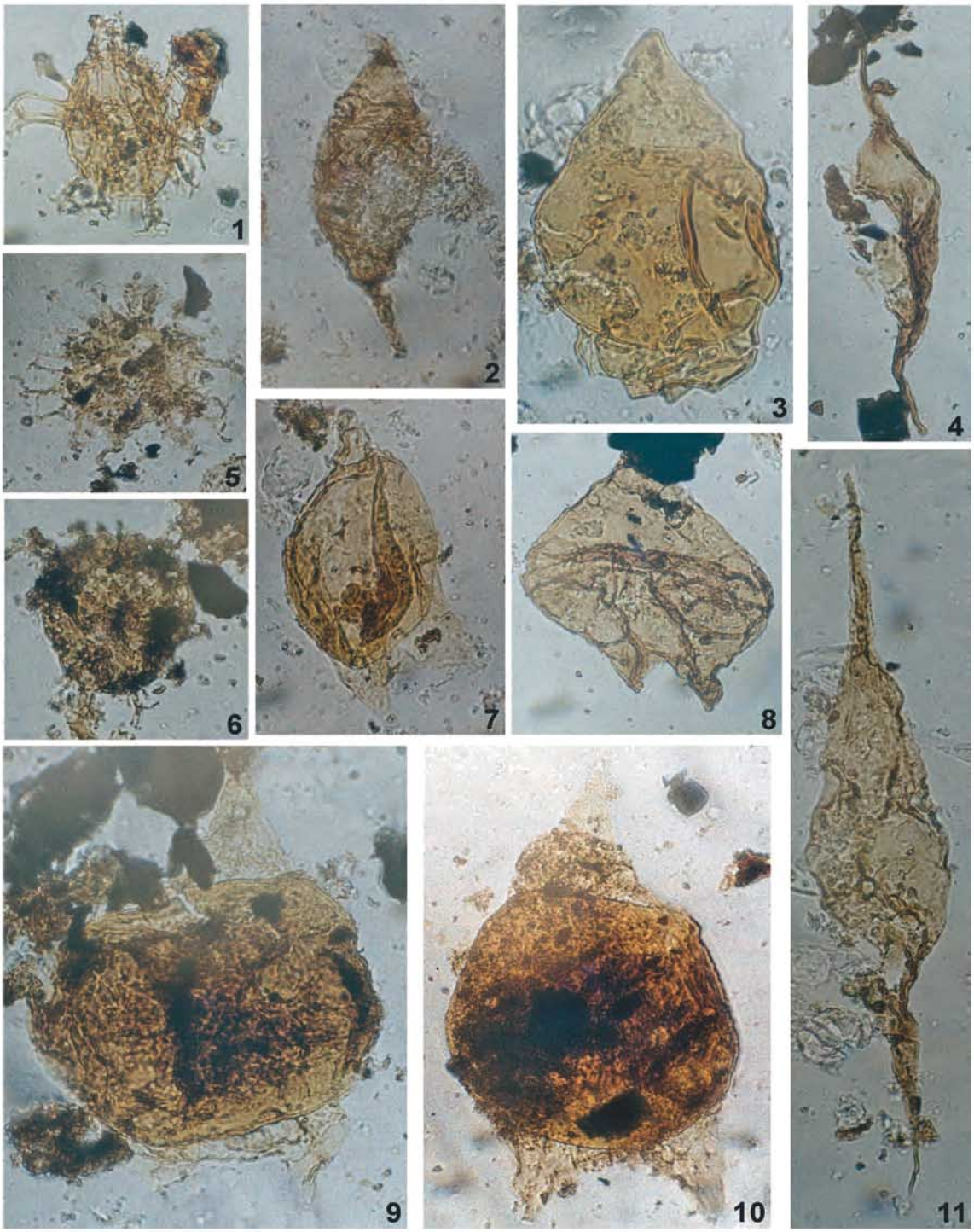

FIG. 7. Dinoflagellate cysts from Cabo Nariz. All photomicrographs were taken using conventional light microscopy. Magnification *ca.*x500. **1**. *Achomosphaera ramulifera* (Deflandre, 1937) Evitt, 1963; **2**. *Palaeocystodinium australinum* (Cookson, 1965) Lentin and Williams, 1976; **3**. *Isabelidinium cooksoniae* (Alberti, 1959) Lentin and Williams, 1977; **4**. *Palaeocystodinium lidiae* (Gorka, 1963) Davey, 1969; **5**. *Hystrichoshpaeridium salpingophorum* Deflandre, 1935; **6**. *Hafniasphaera septata* (Cookson and Eisenack, 1967) Hansen, 1977; **7**. *Isabelidinium* sp.; **8**. *Phelodinium magnificum* (Stanley, 1965) Stover and Evitt, 1978; **9, 10**. *Cerodinium depressa* (Morgenroth, 1966) Lentin and Williams, 1977; **11**. *Palaeocystodinium golzowense* (Alberti, 1961).

TABLE 4. OCCURRENCE OF DINOFLAGELLATE SPECIES ENCOUNTERED IN THE CABO NARIZ AREA.

GENUS	CN06-7	CN06-8	CN05-2	CN04-2	CN06-2
ISABELIDINIUM cooksoniae (Alberti, 1959) Lentin and Williams, 1977	X				
ISABELIDINIUM majae Schioler, 1993	X	X			
HYSTRICHOSPHAERIDIUM salpingophorum Deflandre, 1935	X				
PHELODINIUM magnificum (Stanley, 1965) Stover and Evitt, 1978		X			
PHELODINIUM kozlowskii (Gorka, 1963) Lindrgen, 1984		X			
ACHOMOSPHAERA ramulifera (Deflandre, 1937) Evitt, 1963		X			
PALAEOCYSTODINIUM denticulatum Alberti, 1961		X		X	
PALAEOCYSTODINIUM spp.		X	X		
SENEGALIDINIUM obscura (Drugg, 1967) Williams *et al.* 1998		X			
DEFLANDREA galeata (Lejeune-Carpentier, 1942) Lentin and Williams, 1973		X			
HAFNIASPHAERA septata (Cookson and Eisenack, 1967) Hansen, 1977			X		
CERODINIUM depressa (Morgenroth, 1966) Lentin and Williams, 1977			X		
PALAEOCYSTODINIUM lidiae (Gorka, 1963) Davey, 1969			X		
IMPAGIDINIUM spp.			X		
HYSTRICHOSPHAERIDIUM salpingophorum Deflandre, 1935				X	
CERODINIUM speciosum (Alberti, 1959) Lentin and Williams, 1975				X	
PALAEOCYSTODINIUM australinum (Cookson, 1965) Lentin and Williams, 1976					X
PALAEOCYSTODINIUM golzowense Alberti, 1961					X
DEFLANDREA spp.					X

Palaeocene to Cretaceous with two prominent peaks and a number of lesser age groupings. The youngest age peak comprises 12 analyses with a weighted mean $^{206}Pb/^{238}U$ age of 57.6±1 Ma. A group of 16 analyses forms a prominent peak with a weighted mean age of 74.8±1 Ma. In this case, the younger detrital zircon peak indicates this member to be not older than 57.6 Ma (Thanetian). As noted in figure 8, there is a prominent gap in zircon ages for sample CN06-1 (upper member) between 60 and 70 Ma.

The combined data (fossil record and radiometric age) for the Cabo Nariz Beds, therefore, allows this unit to be assigned an age ranging from Selandian (lower member) to Thanetian or younger (upper member).

6. Structure and the Early Stages of Foreland Evolution in Tierra del Fuego

An interpreted structural cross section of the study area is presented in figure 9. Because the Yartou Thrust juxtaposes Cretaceous with Cenozoic rocks, at first, one may consider this to be the equivalent of the Vicuña Thrust, which is interpreted both by Álvarez-Marrón *et al.* (1999) and Rojas and Mpodozis (2006) (Fig. 3) as the thrust of the Magallanes fold-and-thrust belt closest to the craton, representing its contact with the Cenozoic foreland area. However, given the Paleogene age for the footwall at Cabo Nariz and the fact that structures become shallower northwestwards (Rojas and Mpodozis, 2006; Fig. 3), we favour a link in which the Yartou Thrust may be considered to represent the northwestward continuation of the Colo-Colo thrust, the later name as used in Rojas and Mpodozis (2006).

Because thermal maturity in the area follows a 'normal' pattern, in which the older rock samples have a minor Kübler Index (KI) value (Sánchez *et al.*, 2005), thrusting of the Cerro Cuchilla Formation over the Cabo Nariz Beds occurred after the rocks reached their higher temperature due to either sedimentary loading (between 3 to 6 km for a gradient of 33°C/km), or thick-skin tectonic load, or both. According to Álvarez-Marrón *et al.* (1993), the Cenozoic comprises up to 5,000 m of sedimentary rocks in the foreland area, including Ballena (Paleocene-Eocene) and Bahía Inútil (Oligocene) Groups, so that thrusting of the Cerro Cuchilla Formation over the Cabo Nariz Beds, may have occurred during or after the deposition of the latter unit.

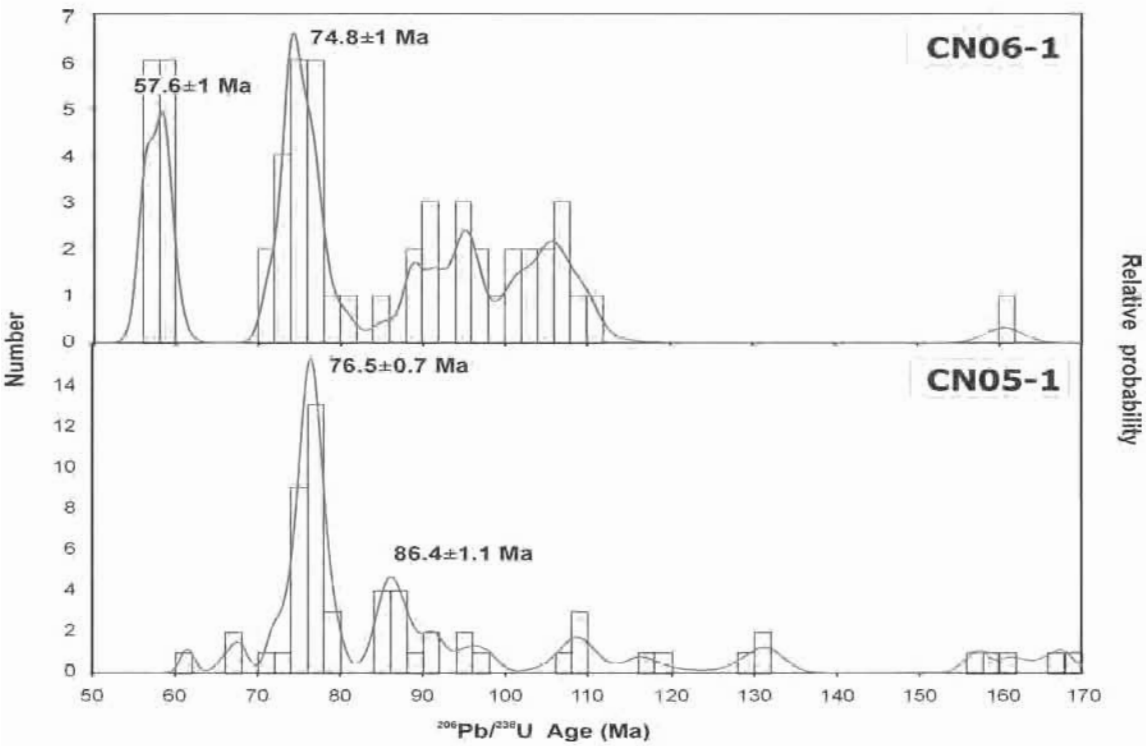

FIG. 8. Relative probability of U-Pb ages of detrital zircons from the Cabo Nariz Beds. The youngest peak in the upper member is 57.6±1 Ma, and in the lower member 76.5±0.7 Ma. Note that in the lower member, there are only 3 zircons with ages between 60 and 70 Ma whereas in the upper member there is a gap between these ages.

7. Sedimentary dikes

Clastic dikes have been reported in all sedimentary environments, but most commonly in deep marine facies (Jolly and Lonergan, 2002). Along the western part of the study area several sedimentary dikes cut the stratified units. They were grouped according to the stratigraphic succession they cut. The attitude of 21 dikes was measured: 6 in the Cerro Cuchilla Formation and 15 in the Cabo Nariz Beds. In figure 5, directional plots are shown for each unit, and a difference in the main orientation of the dikes is clear: N8°W prevails in the Cerro Cuchilla Formation and N42°E in the Cabo Nariz Beds.

According to Suppe (1985), the preferred orientation of dikes may be due to a tectonic control during emplacement, as they develop perpendicular to σ_3. Another possibility is that the attitude difference between the dikes is due to differential tectonic rotation of the blocks: the southern rotated clockwise over the northern one. But as no change in the attitude of the strata is found between these blocks, we postulate that a change in the orientation of σ_3 occurred from Campanian-Danian times to the Thanetian, at least in the Cabo Nariz area.

8. Conclusions and implications

The new data presented here allow several conclusions:

1. The new paleontological and U-Pb ages for the Cabo Nariz area confirm that the Cerro Cuchilla Formation is of Late Campanian-Danian age as reported earlier by ENAP geologists. The footwall Cabo Nariz Beds, are Middle to Late Paleocene in age.
2. The coarsening upward trend in the Cabo Nariz Beds and the paleocurrent data, suggest a north-northwest progradation of a submarine fan over the basin floor.
3. A change in the stress field is shown by the orientation of clastic dikes. This occurred from later Cretaceous-Danian to Thanetian times.
4. The detrital zircon age pattern suggests that there was a lull or a period with reduced magmatic activity in the source area between 70 and 60 Ma.

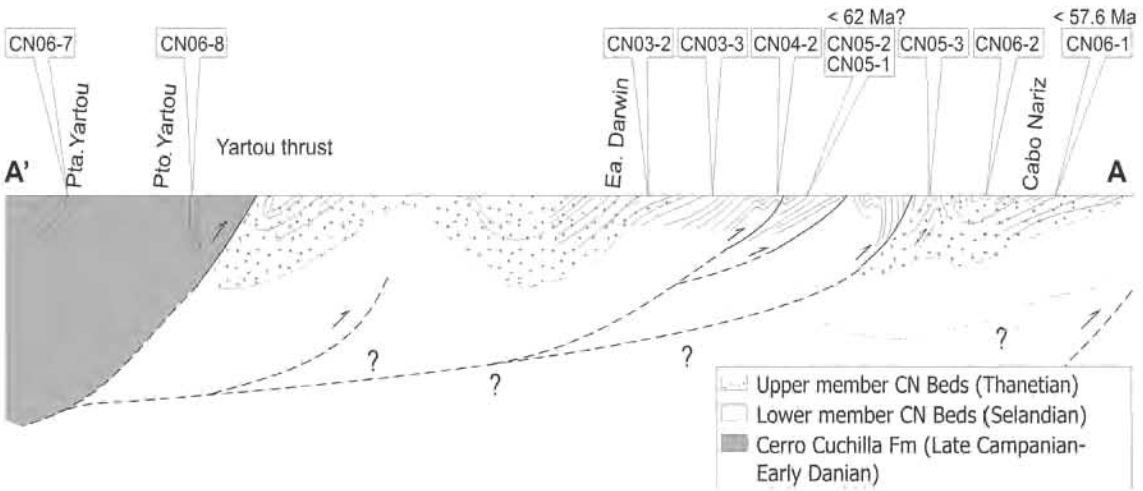

FIG. 9. Tectonic profile at Cabo Nariz and sample location. The thrust under A (not at surface) may correspond to the Vicuña Thrust of Rojas and Mpodozis (2006). Profile after Céspedes (1971)[1].

The north to northwest submarine fan progradation over the basin floor, as well as the change in the stress field (revealed by sedimentary dike orientation) during Middle Paleocene times, suggest a change in tectonic regime as well as a contemporaneous uplift southwards into the study area.

Acknowledgments.

We thank L. Rojas from Empresa Nacional del Petróleo (ENAP) for access to unpublished ENAP reports and A. Carpinelli (ENAP) for logistic support. M. Fuentealba assistance in the field, as well as geologic discussions, and friendship was very important during fieldwork. We also thank Mr. S. Maldonado, the Ea. Miguelito owner, for his support in the field in critical moments. Comments by S. Palma (Universidad de Concepción), C. Mpodozis (Sipetrol, presently at Antofagasta Minerals) and specially J. Le Roux (Universidad de Chile) were useful to improve the manuscript. The project was financed by FONDECYT grants 1010412 and 1050431.

References

Álvarez-Marrón, J.; McClay, K.R.; Harambour, S.; Rojas, L.; Skármeta, J. 1993. Geometry and evolution of the frontal part of the Magallanes Foreland Thrust and fold belt (Vicuña area), Tierra del Fuego, southern Chile. American Association of Petroleum Geologists Bulletin 77 (11): 1904-1921.

Black, L.P.; Kamo, S.L.; Allen, C.M.; Aleinikoff, J.N.; Davis, D.W.; Korsch, R.J.; Foudoulis, C. 2003. TEMORA 1: a new zircon standard for Phanerozoic U-Pb geochronology. Chemical Geology 200: 155-170.

Biddle, K.T.; Uliana, M.A.; Mitchum, R.M.J.; Fitzgerald, M.G. 1986. The stratigraphic and structural evolution of the central and eastern Magallanes Basin, southern South America. *In* Foreland Basins (Allen, P.A.; Homewood, P.; editors). International Association of Sedimentologists Special Publication 8: 41-61.

Fildani, A.; Cope, T.; Graham, S.; Wooden, J. 2003. Initiation of the Magallanes foreland basin: timing of the southernmost Patagonian Andes orogeny revised by detrital zircon provenance analysis. Geology 31: 1081-1084.

Ghiglione, M.; Ramos, V. 2005. Progression of deformation and sedimentation in the southernmost Andes. Tectonophysics 405: 25-46.

Gradstein, F.; Ogg, J.; Smith, A. (editors). 2004. A Geologic Time Scale 2004. Cambridge University Press: 589 p. Cambridge.

Gust, D.; Biddle, K.; Phelps, D.; Uliana, M. 1985. Associated middle to late Jurassic volcanism and extension in southern South America. Tectonophysics 116: 223-253.

Jolly, R.; Lonergan, L. 2002. Mechanisms and controls on the formation of sand intrusions. Journal of the Geological Society 159: 605-617. London.

Lentin, J.K.; Williams, G.L. 1973. Fossil Dinoflagellates: Index to Genera and Species. Geological Survey of Canada, Paper (73-42): 176 p.

Ludwig, K.R. 2001. SQUID 1.02, A User's Manual. Berkeley Geochronology Center, Special Publication 2: 22 p.

Ludwig, K.R. 2003. User's manual for Isoplot/Ex rev. 3.00: a Geochronological Toolkit for Microsoft Ex-

cel. Special Publication 4, Berkeley Geochronology Center, Berkeley: 70 p.

Malumián, N.; Masiuk, V. 1976. Foraminíferos de la Formación Cabeza de León (Cretácico Superior, Tierra del Fuego, República Argentina). Revista de la Asociación Geológica Argentina 31 (3): 180-202.

Martinioni, D.R.; Olivero, E.B.; Palamarczuck, S. 1998. Conglomerados del Paleógeno en Tierra del Fuego: evidencias de discordancia entre el Cretácico Superior-(Paleoceno) y el Eoceno de Cuenca Austral. *In* Paleógeno de América del Sur y de la península Antártica (Casadío, S.; editor). Asociación Paleontológica Argentina, Publicación Especial 5: 129-136.

Martinioni, D.R.; Olivero, E.B.; Palamarczuck, S. 1999. Estratigrafía y discordancias del Cretácico Superior-Paleoceno en la región central de Tierra del Fuego. Simposio 'Paleógeno de América del Sur' (Náñez, C.; editor). Servicio Geológico Minero Argentino, Anales 33: 7-16.

Natland, M.L.; González, P.E.; Cañón, A.; Ernst, M. 1974. A system of stages for correlation of Magallanes basin sediments. Geological Society of America, Memoir 139: 1-126.

Olivero, E.B.; Malumián, N.; Palamarczuk, S.; Scasso, R.A. 2002. El Cretácico Superior-Paleógeno del área del Río Bueno, costa atlántica de la isla Grande de Tierra del Fuego. Revista de la Asociación Geológica Argentina 57 (3): 199-218.

Olivero, E.; Malumián, N.; Palamarczuk, S. 2003. Estratigrafía del Cretácico Superior-Paleoceno del área de Bahía Thetis, Andes fueguinos, Argentina: acontecimientos tectónicos y paleobiológicos. Revista Geológica de Chile 30 (2): 245-263.

Olivero, E.; Malumián, N. 2008. Mesozoic-Cenozoic stratigraphy of the Fuegian Andes, Argentina. Geológica Acta 6: 5-18.

Pavlishina, P.; Sánchez, A.; Hervé, F.; Godoy, E. 2008. New palynological evidences on the presence of latest Cretaceous-Paleocene rocks at the foreland succession at Cabo Nariz, Tierra del Fuego, Chile. *In* Congreso Geológico Argentino, No. 17, Actas 3: 1034-1035. Jujuy.

Prieto, X.; Moraga, J. 1990. El Terciario Inferior de los ríos Rasmussen y Catalina, Tierra del Fuego, Magallanes. *In* Simposio sobre el Terciario de Chile, No. 2, Actas: 259-266. Concepción.

Rojas, L.; Mpodozis, C. 2006. Geología estructural de la Faja Plegada y Corrida del sector chileno de Tierra del Fuego, Andes patagónicos australes. *In* Congreso Geológico Chileno, No. 11, Actas 1: 325-328. Antofagasta.

Sambridge, M.S.; Compston, W. 1994. Mixture modeling of multi-component data sets with application to ion-probe zircon ages. Earth and Planetary Science Letters 128: 373-390.

Sánchez, A.; Belmar, M.; Godoy, E.; Hervé, F. 2005. Cristalinidad de la ilita en limolitas del Cretácico Superior-Paleoceno en Cabo Nariz, Tierra del Fuego. *In* Congreso Geológico Argentino, No. 16, Actas CD-ROM, Artículo 242: 8 p.

Stover, L.E.; Brinkhuis, H.; Damassa, S.P.; de Verteuil, L.; Helby, R.J.; Monteil, E.; Partridge, A.D.; Powell, A.J.; Riding, J.B.; Smelror, M.; Williams, G.L. 1996. Mesozoic-Tertiary dinoflagellates, acritarchs and prasinophytes. *In* Palynology: Principles and Applications (Jansonius, J.; McGregor, D.C.; editors). American Association Stratigraphic Palynologists Foundation 2: 641-750. Dallas.

Suárez, M.; Hervé, M.; Puig, A. 1985. Hoja Isla Hoste e islas adyacentes, XII Región. Servicio Nacional de Geología y Minería, Carta Geológica de Chile 65: 106 p., escala 1:250.000.

Suppe, J. 1985. Principles of Structural Geology. Prentice-Hall: 537 p. New Jersey.

Tera, F.; Wasserburg, G. 1972. U-Th-Pb systematics in three Apollo 14 basalts and the problem of initial Pb in lunar rocks. Earth and Planetary Science Letters 14: 281-304.

Torres-Carbonell, P.; Olivero, E.; Dimieri, L. 2008. Control en la magnitud de desplazamiento de rumbo del Sistema Transformante Fagnano, Tierra del Fuego, Argentina. Revista Geológica de Chile 35 (1): 63-77.

Williams, G.L.; Bujak, J.P. 1985. Mesozoic and Cenozoic dinoflagellates. *In* Plankton Stratigraphy (Bolli, H.M.; Saunders, J.B.; Perch-Nielsen, K.; editors). Cambridge University Press: 847-964.

Williams, I.S. 1998. U-Th-Pb Geochronology by Ion Microprobe. *In* Applications of microanalytical techniques to understanding mineralizing processes (Mc Kibbens, M.A.; Shanks, W.C.; editors). Reviews in Economic Geology 7: 1-35.

Williams, G.L.; Lentin, J.K.; Fensome, R.A. 1998. The Lentin and Williams index of fossil dinoflagellates. American Association of Stratigraphic Palynologists, Contribution Series 34: 1-817.

Wilson, T. 1991. Transition from a back-arc to foreland basin development in the southernmost Andes: Stratigraphic record from the Última Esperanza District, Chile. Geological Society of America, Bulletin 103: 98-111.

Manuscript received: February 11, 2009; revised/accepted: May 04, 2009.